Effects of chronic and acute lead treatments on the biophysical properties of erythrocyte membranes, and a comparison with model membranes☆

Hasna Ahyayauch[a,c,1], Wafae Sansar[b,1], Adela Rendón-Ramírez[a], Félix M. Goñi[a,*], Mohammed Bennouna[b], Halima Gamrani[b]

[a]Unidad de Biofísica (CSIC-UPV/EHU), and Departamento de Bioquímica, Universidad del País Vasco, Bilbao, Spain
[b]Laboratory of Neurosciences, Cadi Ayyad University, Faculty of Sciences Semlalia, Marrakech BP 2390, Morocco
[c]Institut de Formation aux Carrières de Santé de Rabat (IFCSR). Avenue Hassan II, Kilomètre 4,5 Rabat, 10000 Maroc

ARTICLE INFO

ABSTRACT

Rat erythrocytes, or erythrocyte membrane ghosts, have been subjected to either chronic (drinking water containing 15 mM lead acetate for 3 months) or acute (10^{-9}–10^{-2} M lead acetate for 1 h) Pb^{2+} treatments and subsequent changes in membrane properties have been measured. Pb^{2+} concentration in chronically treated rat plasma was 1.8 μM, which is one order of magnitude above normal values. Membrane permeability, or hemolysis, was increased in both cases. A comparative study using liposomes, in the form of large unilamellar vesicles, also indicated an increase in membrane permeability. Membrane microviscosity, or acyl chain molecular order, measured as DPH fluorescence polarization, showed an increased order in the acute treatments, at least below 700 μM Pb^{2+}, and a similar increase in chronically treated rats. The correlation between acute and chronic treatments, and between cell and model membranes, suggests that the present observations may be relevant in the pathogenesis of lead intoxication in humans.

1. Introduction

Lead (Pb) is considered to be a major global environmental health hazard. It is found in nature as a divalent cation, mainly forming stable complexes with sulfur. Pb belongs to the group IVa of the periodic table of elements, it has a relatively large ionic radius (1.2 Å) and a high electronegativity (2.33 in the Pauling scale), which favors its interactions with the coordination groups of proteins [1]. Particularly, the ability of Pb to interact with a flexible coordination number with protein oxygen and sulfur atoms, and to form stable complexes with them, increases its affinity for proteins [2]. Pb is a heavy metal with no known biological function in humans. On the contrary, it can damage various systems of the body including the hematopoietic, renal and skeletal systems, the central nervous system being its primary target [3]. Exposure of the immune system to Pb^{2+} may lead to immunological dysregulation [4]. The susceptibility to Pb^{2+} toxicity is influenced by several factors such as environmental exposure, age and nutritional status. Human exposure to Pb^{2+} occurs via food, water, air and soil [5]. Young children can be easily intoxicated from chronic ingestion of paint chips, house dust or soil containing Pb^{2+} particles. People can also be exposed to Pb^{2+} contamination from industrial sources such as smelters and Pb^{2+} manufacturing industries [5,6]. Also, because Pb^{2+} is a cumulative metal, it constitutes a major hazard for human health. Its toxic effects depend on both the duration of exposure and the magnitude of the dose. The half-life of Pb^{2+} in blood is only 35 days but in the brain it is about 2 years and in bone it persists for decades.

Pb^{2+} intoxication is a complex disorder that affects several cells and organs, including functional and structural alteration of erythrocytes [7,8]. Following exposure, lead is taken up in the bloodstream and transported to other tissues. In human blood, 99% Pb^{2+} is associated with erythrocytes, leaving about 1% in the plasma [9]. The hematological effects result mainly from interference with heme and hemoglobin synthesis, and changes of erythrocyte morphology and survival time result in the anemia frequently observed in Pb^{2+} poisoning [10]. Pb^{2+} is known to have toxic effects on membrane structure and functions [11]. The effects on erythrocyte membranes in particular have been analyzed because erythrocytes have a high affinity for Pb^{2+} and are more vulnerable to oxidative damage than many other cells [12].

The mechanisms underlying Pb^{2+} toxicity are still a matter of research. So far, the effects of Pb^{2+} on Ca^{2+} fluxes and Ca^{2}-regulated

events have been suggested as major mechanisms involved in Pb^{2+} toxicity [13–15]. Other potential mechanisms for Pb^{2+} toxicity include the capacity of Pb^{2+} to affect cell membrane biophysics, however this possibility has not been tested previously, to the authors' knowledge. In our study we have attempted to fill this void in our knowledge of Pb^{2+} toxicology. To this aim we submitted adult male rats to chronic exposure of Pb^{2+} leading to persistently high Pb^{2+} blood levels. The effect of Pb^{2+} on red blood cell hemolysis, morphology and erythrocyte membrane fluidity was investigated. The data were compared with those on cells subjected to an acute Pb^{2+} exposure. Some of the above studies were also repeated on model membranes (large unilamellar liposomes, LUV). A comparison of the three systems, erythrocyte chronic, erythrocyte acute and model membrane, allow important generalisations that may shed light on the biophysical aspects of lead intoxication and are relevant to human exposure to this metal.

2. Materials and methods

2.1. Materials

Egg phosphatidylcholine (PC) was purchased from Lipid Products (South Nutfield, United Kingdom). Diphenylhexatriene (DPH), 1-(4-trimethylammoniumphenyl)-6-phenyl-1,3,5-hexatriene p-toluenesulfonate (TMA–DPH), were from Sigma Aldrich. 8-Aminonaphthalene-1,3,6-trisulfonic acid (ANTS), p-xylene bis (pyridinium bromide) (DPX) were obtained from Molecular Probes Inc. Phosphatidylserine (PS), phosphatidylinositol (PI), and phosphatidic acid (PA) were purchased from Avanti Polar Lipids (Alabaster, Alabama). All other reagents were of analytical quality.

2.2. Animals

Adult male Wistar rats weighing 200 g were raised in the animal house and kept under constant illumination conditions 12:12 light/dark and a room temperature of $22 \pm 3\,°C$. All animals were treated in compliance with the guidelines of the Cadi Ayyad University, Marrakech (Morocco) with adequate measures undertaken to minimize pain and animal discomfort.

Healthy male rats were divided into two groups of 15 animals each. The first group used as controls received distilled water, the second group was treated with drinking water containing 15 mM lead acetate [$Pb^{2+}(CH_3COO)_2\cdot 3H_2O$], dissolved in distilled water. Animals were exposed to this treatment for 3 months according to a previous study [16].

Venous blood samples were collected from rats into heparinised tubes. Blood samples were stored for analyses. Aliquots of blood samples were separated for Pb^{2+} analysis and the remaining blood samples were centrifuged to separate plasma and red blood cells.

2.3. Methods

2.3.1. Preparation of erythrocyte suspensions
Blood was withdrawn from control and Pb^{2+}-treated adult male rats into heparinised tubes. The samples were then centrifuged at 2500xg for 10 min, the plasma obtained was stored at $-25\,°C$, and the pellet washed several times with buffer (144 mM NaCl, 5 mM KCl, 1.8 mM $MgCl_2$, 10 mM Hepes, 5 mM glucose, pH 7.4). To 50 µl erythrocyte suspension 100 µl glutaraldehyde were added for fixation. Fresh blood smears were carried out from 50 µl of control and Pb^{2+}-treated samples and stained with May-Grünwald–Giemsa.

2.3.2. Lead assay
500 µl samples were dissolved in 2.0 ml ultra-pure nitric acid, for atomic absorption spectrometric analysis performed at the ICP AES laboratory, CNRST, Division UATRS, Rabat, Morocco [17].

2.3.3. Iron assay
Iron reacts with chromazurol B (CAB) and cetyltrimethylammoniumbromide (CTMA) to form a coloured ternary complex with an absorbance maximum at 623 nm [18].

2.3.4. Calcium assay
Calcium reacts with methylthymol blue in alkaline medium forming a coloured complex that can be measured by spectrophotometry [19].

2.3.5. Osmolarity assays
A 40 µl aliquot of the diluted control and Pb^{2+}-treated blood sample was measured in an Osmomet 030 osmometer (Gonotec, Berlin).

2.3.6. Hemolysis assays
After centrifugation at 1700xg for 5 min, hemolytic activity was measured as an increase in the A_{412} value (i.e., increase in hemoglobin content) of the supernatant.

2.3.7. Preparation of human erythrocyte ghosts

Blood was collected from healthy donors, placed in EDTA tubes (BD Vacutainer Systems, Franklin Lakes, NJ) and washed with 25 mM HEPES, 150 mM NaCl, pH 7.2 buffer. Right-side-out (RSO) ghosts were prepared following the method of Steck and Kant [20]. Lipid extracts from erythrocyte ghosts in organic solvent were obtained as described previously by Bligh and Dyer [21].

2.3.8. Fluorescence polarization assays

Red blood cells (3.3×10^8 cell/ml) or erythrocyte ghosts (0.3 mM) were incubated with 4 µl fluorescent probe diphenylhexatriene (DPH) for 1 h with stirring and centrifuged at 1600 rpm, 10 min to remove probes that were not incorporated. The fluorescence polarization of DPH and TMA–DPH was measured using a SLM 8100 Spectrofluorometer, equipped with standard polarization accessories and a circulating water bath. The excitation and emission wavelengths were 360 and 430 nm, respectively, for DPH and 365 and 427 nm, respectively, for TMA–DPH. The fluorescence polarization was calculated as:

$$P = \frac{(I_{vv} - G\,I_{vh})}{(I_{vv} + G\,I_{vh})}$$

2.3.8.1. Liposome preparation
The lipids were dissolved in chloroform and mixed as required, and the solvent was evaporated exhaustively. Large unilamellar vesicles were prepared by the extrusion method (10 passages) with filters 0.1 µm in pore diameter [22]. Final lipid concentration was measured as lipid phosphorus.

2.3.8.2. Liposome membrane permeability
Liposome membrane permeability was determined by measuring the efflux of probe previously encapsulated in lipid vesicles. The leakage of vesicular aqueous contents was assayed with ANTS and DPX entrapped in the liposomes according to Ellens et al. [23]. Non-entrapped probe was removed by gel filtration on Sephadex G-25 columns. Fluorescence measurements were carried out in a LS-50B Perkin–Elmer spectrofluorometer, at room temperature (37 °C) and with continuous stirring. The osmolality of intra- and extravesicular solutions was measured in a cryoscopic osmometer (Osmomat 030, Gonotec, Berlin, Germany) and adjusted to 0.3 osm/kg by adding NaCl. An interference filter (520 nm) was used to avoid scattered excitation light. Fluorescence measurements were performed by setting the (ANTS + DPX) emission at 520 nm and the excitation at 355 nm. The 0% leakage corresponded to the fluorescence intensity (F_0) of a suspension containing 100 µM liposomes at time zero; 100% leakage

Table 1
Effects of chronic Pb^{2+} treatment on rats and rat erythrocytes.

	Control	Pb^{2+}-treated
Plasma Pb^{2+} (μM)	0.17 ± 0.08	1.84 ± 0.19
Plasma Ca (mM)	3.5 ± 0.1	1.3 ± 0.1
Plasma Fe (μM)	33.2 ± 0.1	31.0 ± 0.1
Osmolality (mosm)	327 ± 2.0	363 ± 20.1
Hemolysis (relative)	1.0	1.6 ± 0.05
DPH polarisation*	0.204 ± 0.006	0.343 ± 0.033

Average values $\pm$ S.E.M. ($n = 3$–5).
* Erythrocyte ghost membranes.

was the fluorescence value (F_{100}) obtained when LUV are lysed by adding 10 μl Triton X-100 [24]. To test the destabilizing effect of lead the metal was added to liposomal suspensions at different concentrations. Fluorescence of each sample was recorded for 30 min.

The percentage of efflux was calculated by the following equation:

$$F\% = \frac{(F_t - F_0)}{(F_{100} - F_0)} \times 100,$$

where F_0 and F_t are the fluorescence at 530 nm in the absence and in the presence of Pb^{2+}, respectively.

2.3.9. Dynamic light scattering

Dynamic light scattering (DLS) measurements of particle sizes were carried on a Malvern Zetasizer nano System. This instrument was equipped with a 4 mW He–Ne laser of 633 nm wavelength, and an avalanche photodiode detector (quantum efficiency >50% at 633 nm) located at 173° from the incident beam direction in a backscatter position. The temperature of the sample holder was stabilized at 37 °C through a Peltier thermostat. Samples were introduced into plastic 50–2000-μl capacity disposable cuvettes (UVette, Eppendorf, Hamburg, Germany).

3. Results and discussion

3.1. Chronic Pb^{2+} intoxication

Chronic treatments of rats with Pb^{2+} as indicated under 'Methods' caused highly increased plasma lead levels (Table 1). Plasma iron and particularly calcium were concomitantly decreased. Under the same conditions red blood cell osmolality hardly changed, but erythrocyte membranes became more fragile, thus hemolysis increased (Table 1). All the above results are in agreement with the previous similar study by Missoun et al. [25]. Also in Table 1 polarisation of DPH fluorescence emission, considered to reflect molecular membrane order, increased markedly in the intoxicated rats erythrocyte ghosts membranes. Increased membrane order of the extent found here could mean a high degree of membrane rigidity, and the latter to increased hemolysis [26].

The above changes in red blood cells were accompanied by an abnormal morphology, Pb^{2+} stimulated the transition from the normal biconcave shape to echinocyte morphology (Fig. 1B). Erythrocytes larger than normal are also observed (arrows). This is in contrast with the normal morphology of the erythrocytes from control rats (Fig. 1A).

The distribution of toxins, especially Pb^{2+} inside the cells has been the subject of recent studies in one of our laboratories [27,28]. Pb^{2+} affects many organ systems, mainly through its effect on blood. Following exposure, Pb^{2+} is taken up in the bloodstream and transported to other tissues. In blood, 99% of Pb^{2+} is associated with erythrocytes leaving about 1% free in plasma [9,29]. In the present work we provide evidence that Pb^{2+} blood level is increased in chronically treated rats as compared to controls. Chronic Pb^{2+} exposure decreases both the blood calcium and iron levels as compared to
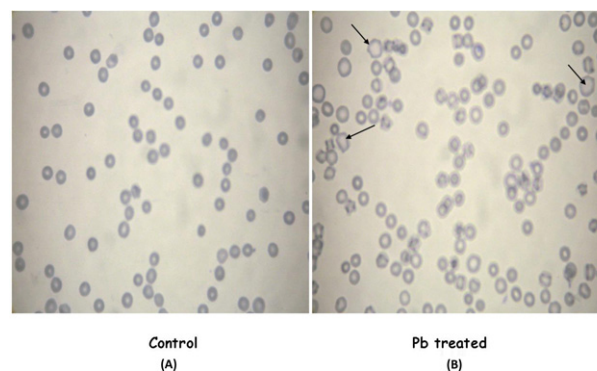
Fig. 1. Erythrocyte morphology of control (A), and chronically intoxicated (B), rats. May-Grünwald–Giemsa stain.

controls. The metabolisms of calcium and lead are similar in certain respects and have a number of potential sites for interaction. It has been reported previously that Pb^{2+} can be transported into the erythrocytes through the Ca^{2+} transport systems and that this might alter calcium homeostasis [30].

3.2. Acute Pb^{2+} intoxication

Properties of red blood cell membranes were examined 1 h after Pb^{2+} addition. Pb^{2+} caused a dose-dependent increase in the number of echinocytes (Fig. 2). At the highest concentrations tested abnormally large red blood cells were also observed. Overall, the morphological changes induced by acute Pb^{2+} intoxication were similar to those observed after chronic intoxication except that, with acute treatments, Pb^{2+} concentrations one or two orders of magnitude higher than in the chronic treatments were required (Fig. 1).

Submicromolar concentrations of lead induced hemolysis, the effect being only moderate (up to 4%) (Fig. 3). Hemolysis increased but slowly with Pb^{2+} concentrations >1 μM. An increased hemolysis was also observed after chronic intoxication (Table 1).

The acute effects of Pb^{2+} on membrane order, measured as polarisation of the fluorescence emission of DPH, were interesting. Pb^{2+} concentrations in the 100–700 μM range increased DPH polarisation (Fig. 4), which is interpreted as an increase in membrane lipid chain order [31]. However when the effect of Pb^{2+} concentrations above 700 μM was considered, a decreased polarisation was observed (Fig. 4), a phenomenon that may involve direct Pb^{2+} interaction with membrane integral proteins. The data below 700 μM Pb^{2+} are in agreement with the clear increase in DPH polarisation observed after chronic lead intoxication (Table 1), only Pb^{2+} concentrations about two orders of magnitude higher were required to produce the same effect with acute treatments. Amoruso et al. [32] also observed an increased DPH polarisation after acute treatment of erythrocytes with Pb^{2+}.

DPH is a highly non-polar molecule, that distributes uniformly within the membrane hydrophobic matrix. TMA–DPH however is an amphipathic molecule, that orients itself at the lipid–water interface, thus providing information on lipid chain order in the region close to the phospholipid headgroups [33]. The acute effects of Pb^{2+} on TMA–DPH polarisation in erythrocyte ghost membrane are shown in Fig. 5. Polarisation (lipid chain order) decreases continuously with Pb^{2+} concentration, the decrease being steeper between 100 and 1000 μM Pb^{2+}. Thus both DPH and TMA–DPH provide complementary information showing that acute treatments with lead concentrations up to 700 μM cause an overall ordering of membrane lipid chains, with a localized disordering in the chain regions close to the interface.

Jang et al. [34] observed that low levels of lead induce phosphatidylserine exposure and erythrophagocytosis, through inhibition
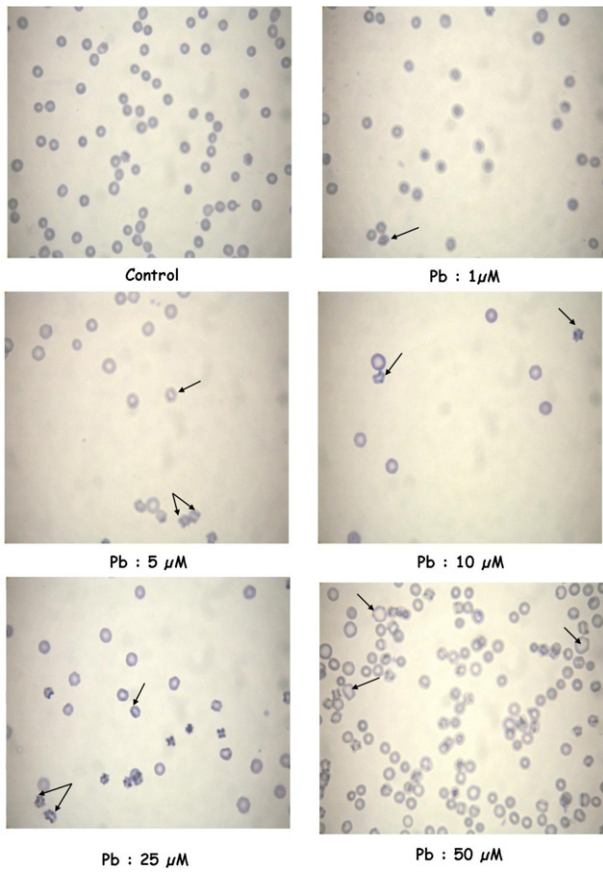
Fig. 2. Erythrocyte morphology of control and acutely intoxicated cells. May-Grunwald–Giemsa stain. The cells were treated for 1 h with the Pb²⁺ concentrations indicated under each picture.
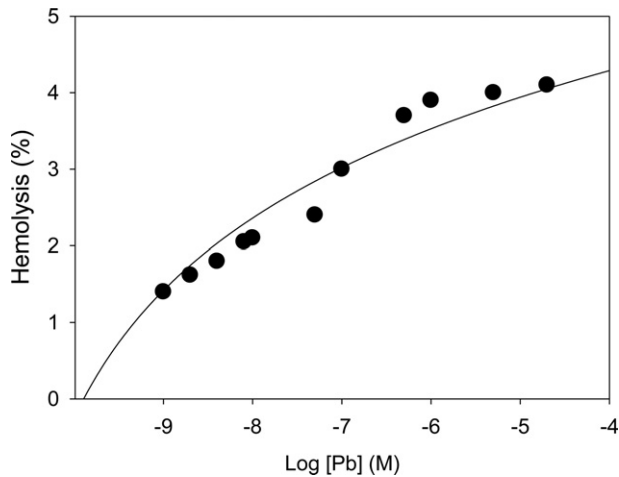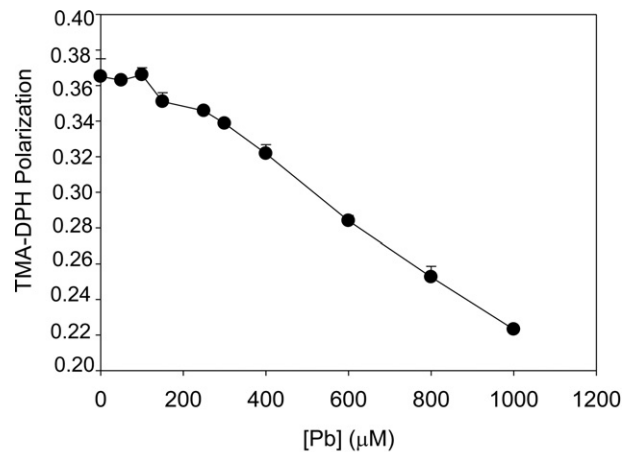

Fig. 3. Hemolysis after acute (1 h) Pb²⁺ treatments. Average of three measurements. S.E.M. roughly the size of the symbols, or smaller.

of the phospholipid translocase flippase. These results were observed both after acute and subchronical Pb²⁺ intoxication. The increased lipid order revealed through increased DPH polarization in both acute and chronical intoxication may be at the origin of the observed hemolysis (Fig. 3) and of splenic sequestration and erythrophagocytosis [34]. Hemolysis secondary to an increased membrane order/rigidity has been observed [26] in a previous study in one of our laboratories.
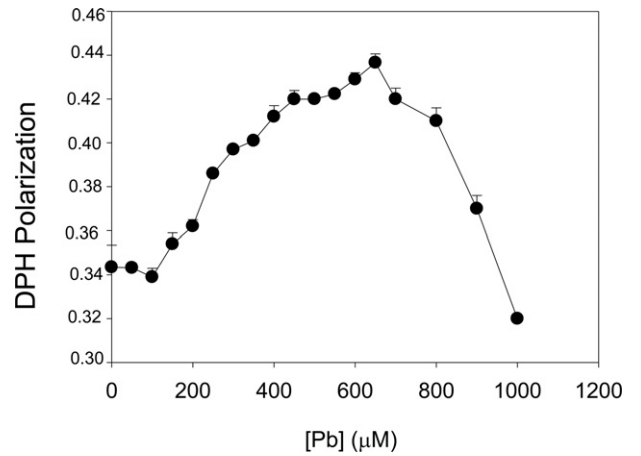
Fig. 4. DPH fluorescence polarisation in erythrocyte ghosts after acute (1 h) Pb²⁺ treatments. Average values ± S.E.M. (n = 3).


Fig. 5. TMA–DPH fluorescence polarisation in erythrocyte ghosts after acute (1 h) Pb²⁺ treatments. Average values ± S.E.M. (n = 3).

3.3. Leakage from lipid vesicles

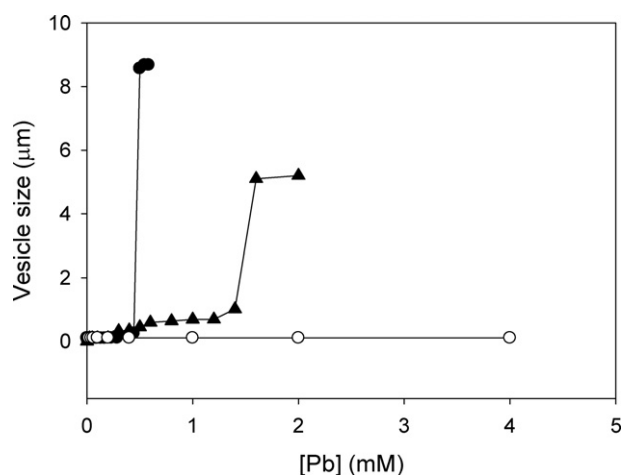As a further effort to understand the molecular effects of Pb²⁺ on membranes a number of studies were carried out with model membranes, namely large unilamellar vesicles (LUV) about 100 nm in diameter. LUV of three different compositions were prepared, namely pure PC, pure PI and PC:PA (8:2 mol ratio). PC is intended to represent the mostly neutral lipid composition of the cell plasma membrane outer monolayer. The negatively-charged PI and PC:PA should provide an increased interaction with the metal.

Liposomal leakage, or release of trapped solutes, was measured looking for a parallel of Pb²⁺-induced hemolysis as seen in Fig. 3, i.e. lead-induced liposomal leakage at the same concentrations that caused hemolysis (Fig. 6). Pb²⁺ was effective on LUV of all three compositions tested, but sensitivity decreased in the order PI > PC:PA > PC. A strict parallelism cannot be established between liposomal leakage and hemolysis, because in the former case the released solutes have a much smaller molecular weight than hemolysis in the latter. Still, it can be qualitatively ascertained that Pb²⁺ increases the permeability of both model and cell membranes.

The hemolysis phenomenon is commonly regarded as connected with the lipid part of the erythrocyte membrane. The agreement found between the results of both sets of studies in erythrocytes and in liposomes provides evidence that Pb²⁺ acts directly on the lipid matrix. However one cannot exclude an action, directly or via the lipid phase, on membrane proteins [35]. Addition of Pb²⁺ to blood causes
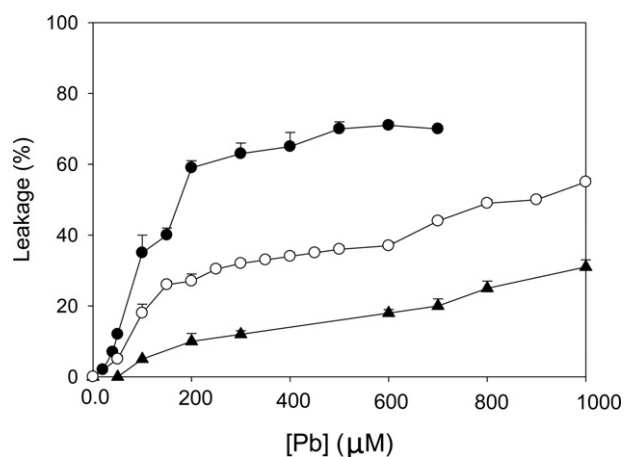
Fig. 6. Pb^{2+} induced release of aqueous liposomal contents. Large unilamellar vesicles of different lipid compositions were used: PC (▲), PC:PA (80:20 mol ratio) (o), or PI (●). Average values ± S.E.M. ($n = 3$).

Fig. 8. Pb^{2+}-induced TMA–DPH fluorescence polarisation in liposomal membranes. LUV composition was: PC (▲), PC:PA (80:20 mol ratio) (o), or PI (●). Average values ± S.E.M. ($n = 3$).
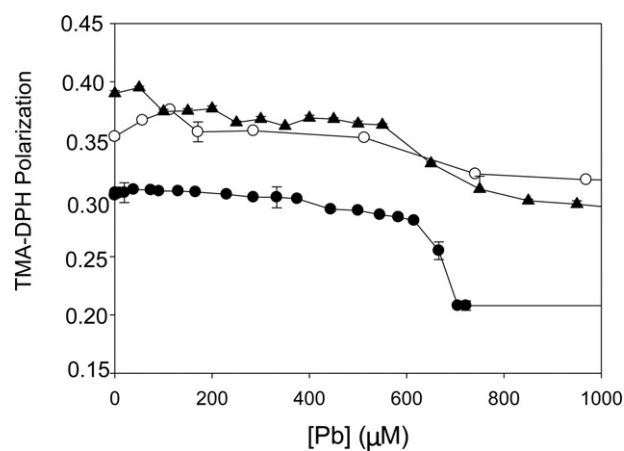

Fig. 7. Pb^{2+}-induced liposome aggregation (increase in particle size) measured by quasi-elastic light scattering as a function of Pb^{2+} concentration. Initial vesicle size was 0.1 μM. LUV composition was PC (▲), PC:PA (80:20 mol ratio) (o), or PI (●). Average of three measurements. S.E.M. roughly the size of the symbols, or smaller.

membrane leakage which means that more water can enter the cell before haemolysis occurs [36]. The changes in erythrocyte shape, observed in this work, may also be related to the interference of Pb^{2+} with Fe found to be decreased at the blood level. Other studies have also demonstrated that micromolar concentrations of Pb^{2+} can permeate the membrane and disrupt the liposome transmembrane pH gradient, resulting in the alkalinization of the intraliposomal aqueous space [37].

3.4. Further liposomal studies

To confirm that the higher effect of Pb^{2+} on negatively-charged vesicles was related to electrostatic interactions the size of Pb^{2+}-vesicle aggregates was measured by quasi-elastic light scattering as a function of lead concentration. The results in Fig. 7 show that Pb^{2+} did not cause aggregation of PC vesicles, while aggregation was observed with PC:PA and even more with PI vesicles, i.e. the same order in which leakage was detected. The data in Fig. 7 confirm the electrostatic interaction of Pb^{2+} and PC:PA or PI liposomes, and suggest that vesicle–vesicle aggregation may help in the Pb^{2+}-induced release of aqueous vesicular contents.

Lead effects on the molecular order of lipids in liposomes were assayed with the amphipathic probe TMA–DPH. With all three LUV

compositions Pb^{2+} was seen to decrease TMA–DPH polarisation, i.e. to decrease membrane order (Fig. 8), in agreement with the erythrocyte ghost observations (Fig. 5). TMA–DPH is located at the lipid–water interface, as discussed above. Perhaps the physical properties in this region of the bilayer are governed mainly by its interfacial nature, independently of the presence or absence of proteins. This would explain the very similar results of TMA–DPH polarisation in erythrocyte ghost membranes (Fig. 5) and in liposomes (Fig. 8). However in the deeper regions of the hydrophobic matrix, that are explored by DPH, the presence of intrinsic proteins with their inherent lipid disordering capacity [38] would interfere with the effects of Pb^{2+}, not excluding direct Pb^{2+}–protein interactions, giving rise to a more complex DPH polarisation response.

4. Concluding remarks

The above results demonstrate the capacity of Pb^{2+} to affect cell membrane biophysics. This aspect of lead toxicology has hardly been considered in earlier studies. Three different systems have been studied, namely chronically exposed erythrocytes, acutely exposed erythrocytes, and model membranes (LUV). A comparison of the different results allows us to conclude that in all cases lead: (i) increases membrane permeability, (ii) increases the overall membrane lipid order (at the toxicologically relevant concentrations), and (iii) alters erythrocyte morphology, giving rise to macrocytic and echinocytic forms. Pb^{2+} effects on red blood cells after acute treatments reproduce faithfully the effects of chronic intoxication except that acute effects require lead concentrations 2–3 orders of magnitude higher. Liposomes exhibit a similar sensitivity to Pb^{2+} than erythrocytes in acute treatments. The parallelism between membrane effects of Pb^{2+} in the three systems under study reflects that the data are relevant to human intoxication by lead. In particular the observation that exposure to low (1–2 μM) Pb^{2+} concentrations for extended periods of time has the same effects on membranes to that of acute treatments with 50–500 μM Pb^{2+} supports the contention that the data in this paper can be at the origin of certain signs, e.g. anemia, of lead intoxication in humans.

Conflicts of interest

The authors declare no conflicts of interest related to this paper.

Acknowledgments

References

[1] Godwin H.A. (2001) The biological chemistry of lead. Curr. Opin. Chem. Biol. 5, 223–227.

[2] Garza A., Vega R., Soto E. (2006) Cellular mechanisms of lead neurotoxicity. Med. Sci. Monit. 12, RA57–RA65.

[3] Wilson M.A., Johnston M.V., Goldstein G.W., Blue M.E. (2000) Neonatal lead exposure impairs development of rodent barrel field cortex. Proc. Natl. Acad. Sci. U S A. 97, 5540–5545.

[4] Fang L., Zhao F., Shen X., Ouyang W., Liu X., Xu Y. et al. (2012) Pb^{2+} exposure attenuates hypersensitivity in vivo by increasing regulatory T cells. Toxicol. Appl. Pharmacol. 265, 272–278.

[5] White L.D., Cory-Slechta D.A., Gilbert M.E., Tiffany-Castiglioni E., Zawia N.H., Virgolini M. et al. (2007) New and evolving concepts in the neurotoxicology of lead. Toxicol. Appl. Pharmacol. 225, 1–27.

[6] Goyer R.A. (1996) Results of lead research: prenatal exposure and neurological consequences. Environ. Health Perspect. 104, 1050–1054.

[7] Koller K., Brown T., Spurgeon A., Levy L. (2004) Recent developments in low-level lead exposure and intellectual impairment in children. Environ. Health Perspect. 112, 987–994.

[8] Calderón-Salinas J.V., Quintanar-Escorcia M.A., González-Martínez M.T., Hernández-Luna C.E. (1999) Lead and calcium transport in human erythrocyte. Hum. Exp. Toxicol. 18, 327–332.

[9] Schütz A., Bergdahl I.A., Ekholm A., Skerfving S. (1996) Measurement by ICP-MS of lead in plasma and whole blood of lead workers and controls. Occup. Environ. Med. 53, 736–740.

[10] Terayama K. (1993) Effects of lead on electrophoretic mobility, membrane sialic acid, deformability and survival of rat erythrocytes. Ind. Health 31, 113–126.

[11] Donaldson W.E., Knowles S.O. (1993) Is lead toxicosis a reflection of altered fatty acid composition of membranes? Comp. Biochem. Physiol. C. 104, 377–379.

[12] Rendón-Ramirez A., Cerbón-Solórzano J., Maldonado-Vega M., Quintanar-Escorza M.A., Calderón-Salinas J.V. (2007) Vitamin-E reduces the oxidative damage on delta-aminolevulinic dehydratase induced by lead intoxication in rat erythrocytes. Toxicol In Vitro. 21, 1121–1126.

[13] Bressler J., Kim K.A., Chakraborti T., Goldstein G. (1999) Molecular mechanisms of lead neurotoxicity. Neurochem. Res. 24, 595–600.

[14] Marchetti C. (2003) Molecular targets of lead in brain neurotoxicity. Neurotox. Res. 5, 221–236.

[15] Toscano C.D., Guilarte T.R. (2005) Lead neurotoxicity: from exposure to molecular effects. Brain Res. Rev. 49, 529–554.

[16] Lasley S.M., Green M.C., Gilbert M.E. (2001) Rat hippocampal NMDA receptor binding as a function of chronic lead exposure level. Neurotoxicol. Teratol. 23, 185–189.

[17] Franzblau A., Rosenstock L., Eaton D.L. (1988) Use of inductively coupled plasma-atomic emission spectroscopy (ICP-AES) in screening for trace metal exposures in an industrial population. Environ. Res. 46, 15–24.

[18] Garcic A. (1979) A highly sensitive, simple determination of serum iron using chromazurol B. Clin. Chim. Acta 94, 115–119.

[19] Barnett R.N., Skodon S.B., Goldberg M.H. (1973) Performance of "kits" used for clinical chemical analysis of calcium in serum. Am. J. Clin. Pathol. 59, 836–845.

[20] Steck T.L., Kant J.A. (1974) Preparation of impermeable ghosts and inside-out vesicles from human erythrocyte membranes. Methods Enzymol. 31, 172–180.

[21] Bligh E.G., Dyer W.J. (1959) A rapid method of total lipid extraction and purification. Can. J. Biochem. Physiol. 37, 911–917.

[22] Mayer L.D., Hope M.J., Cullis P.R. (1986) Vesicle of variable sized produced by a rapid extrusion procedure. Biochim. Biophys. Acta 858, 161–168.

[23] Ellens H., Bentz J., Szoka F.C. (1984) pH-induced destabilization of phosphatidylethanolamine-containing liposomes: role of bilayer contact. Biochemistry 23, 1532–1538.

[24] Ahyayauch H., Bennouna M., Alonso A., Goñi F.M. (2010) Detergent effects on membranes at subsolubilizing concentrations: transmembrane lipid motion, bilayer permeabilization, and vesicle lysis/reassembly are independent phenomena. Langmuir 26, 7307–7313.

[25] Missoun F., Slimani M., Aoues A. (2010) Toxic effect of lead on kidney function in rat Wistar. African J. Biochem. Res. 4, 21–27.

[26] Montes L.R., López D.J., Sot J., Bagatolli L.A., Stonehouse M.J., Vasil M.L. et al. (2008) Ceramide-enriched membrane domains in red blood cells and the mechanism of sphingomyelinase-induced hot-cold hemolysis. Biochemistry 47, 11222–11230.

[27] Bouyatas M.M., Gamrani H. (2007) Immunohistochemical evaluation of the effect of lead exposure on subcommissural organ innervation and secretion in Shaw's Jird (Meriones shawi). Acta Histochem. 109, 421–427.

[28] Sansar W., Ahboucha S., Gamrani H. (2011) Chronic lead intoxication affects glial and neural systems and induces hypoactivity in adult rat. Acta Histochem. 113, 601–607.

[29] Cake K.M., Bowins R.J., Vaillancourt C., Gordon C.L., McNutt R.H., Laporte R. et al. (1996) Partition of circulating lead between serum and red cells is different for internal and external sources of lead. Am. J. Ind. Med. 29, 440–445.

[30] Quintanar-Escorza M.A., González-Martínez M.T., Navarro L., Maldonado M., Arévalo B., Calderón-Salinas J.V. (2007) Intracellular free calcium concentration and calcium transport in human erythrocytes of lead-exposed workers. Toxicol. Appl. Pharmacol. 220, 1–8.

[31] Lentz B.R. (1993) Use of fluorescent probes to monitor molecular order and motions within liposome bilayers. Chem. Phys. Lipids 64, 99–116.

[32] Amoruso M.A., Witz G., Goldstein B.D. (1987) Alteration of erythrocyte membrane fluidity by heavy metal cations. Toxicol. Ind. Health 3, 135–144.

[33] Prendergast F.G., Haugland R.P., Callahan P.J. (1981) 1-[4-(Trimethylamino)phenyl]-6-phenylhexa-1,3,5-triene: synthesis, fluorescence properties, and use as a fluorescence probe of lipid bilayers. Biochemistry 20, 7333–7338.

[34] Jang W.H., Lin K.M., Kim K., Noh J.Y., Kang S., Chang Y.K. et al. (2011) Low level of lead can induce phosphatidylserine exposure and erythrophagocytosis. Toxicol. Sci. 122, 177–184.

[35] Trela Z., Radecki J., Prezestalski S. (1997) Effect of triphenyl lead chloride on the resting potential and electrical conductance of Nitellopsisobtusa membrane. Poll. J. Environ. Stud. 4, 37–40.

[36] Griggs R.C. (1964) Lead poisoning: Hematologic aspects. Prog. Hematol. 4, 117–137.

[37] Díaz R.S., Monreal J. (1995) Protein-independent lead permeation through myelin lipid liposomes. Mol. Pharmacol. 47, 766–771.

[38] Chapman D., Gómez-Fernández J.C., Goñi F.M. (1979) Intrinsic protein–lipid interactions. Physical and biochemical evidence. FEBS Lett. 98, 211–223.